Global J. Environ. Sci. Manage. 9(4): 741-752, Autumn 2023, Serial #36

Global Journal of Environmental Science and Management
(GJESM)

Homepage: https://www.gjesm.net/

Podcasts

ORIGINAL RESEARCH PAPER

Exploring the dynamics of seasonal surface features using coastal and regional ocean community model

D. Jaishree[1,*], P.T. Ravichandran[1], D.V. Thattai[2]

[1] *Department of Civil Engineering, Faculty of Engineering and Technology, SRM Institute of Science and Technology, Kattankulathur 603203, Chengalpattu District, Tamil Nadu, India*

[2] *Indira Nagar, Adyar, Chennai 600 020, Tamil Nadu, India*

ARTICLE INFO

Article History:
Received 09 December 2022
Revised 23 March 2023
Accepted 23 April 2023

Keywords:
Bay of Bengal (BoB)
Coastal and Regional Ocean Community model
Depth of the Isothermal Layer-D20 and D26
Net heat flux
Numerical model
Salinity
Temperature

DOI: 10.22035/gjesm.2023.04.06

ABSTRACT

BACKGROUND AND OBJECTIVES: Studying the monthly variations in the surface features of the Bay of Bengal is a complex task that involves numerous large-scale ocean-atmosphere dynamics. This study identified the bay's changing circulation patterns over recent decades as a crucial study area requiring in-depth research. Understanding the changes in circulation patterns provides valuable insights into the Bay dynamics. It helps identify the potential impacts of climate change, ocean currents, and other factors on the bay's ecosystem. This study aims to understand the seasonal variability of the Bay of Bengal's surface circulation features using a high-resolution numerical Coastal and Regional Ocean Community simulations model.
METHODS: To conduct the study in the Bay of Bengal, the Coastal and Regional Ocean Community model, a numerical ocean model, was utilized. The high-resolution numerical model for ocean circulation is three-dimensional and uses hydrostatic primitive equations in generalized curvilinear coordinates. Simulations were conducted over 8 years using a grid comprising 256 x 249 horizontal surface points to model a range of ocean-atmospheric parameters. This grid provided an approximate resolution of 10 kilometers.
FINDINGS: The findings are based on the model's enhanced performance compared to previous study results. It was observed that the sea surface temperature remains above 28 degrees Celsius throughout the bay except in winter. During the monsoon season, surface salinity was observed to be reduced in the Bay of Bengal's northern region and western and eastern boundaries. Surface eddies along the western bay extend to deep waters before the onset of monsoon. The net heat flux in the bay has been determined as positive before monsoon, negative post-monsoon, and mixed during the monsoon season.
CONCLUSION: This analysis focuses on the ocean surface layer with more prominent dynamics. Various surface parameters were calculated, and discussions on surface temperature, salinity, D20, D26, and net heat flux across seasons have been presented.

NUMBER OF REFERENCES	NUMBER OF FIGURES	NUMBER OF TABLES
49	8	0

*Corresponding Author:
Email: *jaishred@srmist.edu.in*
Phone: +900 3180 202
ORCID: 0000-0003-0401-068X

Note: Discussion period for this manuscript open until January 1, 2024 on GJESM website at the "Show Article".

INTRODUCTION

The Bay of Bengal (BoB) is a large inlet of the Indian Ocean located in the northeastern part of the Indian subcontinent. To the west, India and Sri Lanka form the borders, while Bangladesh is situated to the north. On the eastern side, Myanmar marks the boundary, and the Andaman and Nicobar Islands are closer to the Myanmar boundary. The bay has a total area of approximately 2,172,000 square kilometers (km^2) and a maximum depth of about 5,000 m (meters) (Chakraborty and Gangopadhyay, 2016). Besides significantly impacting regional climate patterns, the BoB is a significant source of fisheries. Its warm waters are home to numerous fish species and other marine life. Additionally, its waters serve as convenient transport with shipping routes between India, Bangladesh, Sri Lanka, and other Southeast Asian countries (De and Carvalho-Junior, 2022; Sharada *et al*., 2015). The potential role of the BoB in climate change has also been extensively investigated (Li *et al*., 2018; Salathe Jr *et al*., 2008). Studies have found that the BOB's large surface area and warm waters can significantly affect regional climate patterns. Moreover, scientific investigations have demonstrated that the BoB, proximal to the equator, can be a potential origin for severe weather phenomena like cyclones. Various facets of the BoB have been explored in studies, including its ecology, fisheries, coastal resources and management, climate change impacts, and oceanography. (Yadav, 2022; Sardessai *et al*., 2007). Research has also been conducted on prevalent topics such as marine pollution, sedimentation processes, sea-level rise, and coastal erosion. The BoB is characteristically tropical and humid, with temperatures ranging from 23 to 32 degrees Celsius (°C). Monsoons bring heavy rains to the region from June to October, while a dry season extends from December to April (Akhter *et al*., 2021; Cherian *et al*., 2020; Potemra *et al*., 1991; Suprit and Neelakandan, 2016). The bay is an important part of the surrounding countries' climate system because it helps drive the monsoon rains, which are essential for agriculture in the region. Monsoons bring heavy rains to India, Bangladesh, and Myanmar during the summer months providing respite from the heat and necessary water for agriculture (June through September). (Jongaramrungruang *et al*., 2017; Krishnamurti *et al*., 2017; Schott and McCreary, 2001; Wainer and Webster, 1996; Webster *et al*., 1998). The BoB plays a significant role in this process by helping to create a low-pressure area over the Indian subcontinent. This low-pressure area draws in moisture from the ocean, resulting in heavy rains over land. Studies have shown that sea surface temperature (SST) changes in the BoB can significantly impact monsoon rainfall patterns. (Bartzokas *et al*., 2018; Dyn, 2010; Gordon *et al*., 2016; Lee *et al*., 2000; Setiawan *et al*., 2022; Vinayachandran *et al*., 2014;). The BoB region is particularly prone to cyclone genesis, with April–December being the typical peak period for cyclone formation. Cyclone genesis in the BoB is closely linked to the region's oceanic and atmospheric conditions (Ali *et al*., 2007; Fan *et al*., 2020; Girishkumar and Ravichandran, 2012; Kikuchi *et al*., 2009; Kodunthirapully Narayanaswami and Ramasamy, 2022; Lin *et al*., 2009). Being one of the warmest waterbodies, with SST often exceeding 30 °C during the peak cyclone season, o cean heating is an important factor contributing to the genesis of hurricanes in the BoB. (Amsalia *et al*., 2022; Echols, 2020; Horii *et al*., 2016; Kawai and Wada, 2007; Segele *et al*., 2009; Sen *et al*., 2021; Thadathil *et al*., 2002; Vecchi and Harrison, 2002; Yoo *et al*., 2010; Yu and Hole, 2015). This warm water provides a significant energy source for the formation and intensification of cyclones, providing the necessary heat and moisture for convective processes. (Jyothi *et al*., 2019) In addition to ocean heating, other factors such as wind shear, atmospheric instability, and pre-existing disturbances also contribute to the origin of cyclones in the BoB. These factors can interact in complex ways, creating conditions required for cyclones to form and intensify. (Maneesha *et al*., 2012; Roy Chowdhury *et al*., 2021; Ts *et al*., 2020). The climatological significance of the cyclones in the bay cannot be overstated. Cyclones in this region can significantly impact the surrounding coastal communities through floods, storm surges, and high winds. (Jourdain *et al*., 2013). In addition, the heavy rainfall associated with cyclones can have significant adverse implications on the region's agriculture and water resources (Ali *et al*., 2007). Given the potential for significant impacts from cyclones in the BoB, monitoring and forecasting these events as accurately as possible is imperative. Accurate forecasting requires a comprehensive understanding of the oceanic and atmospheric conditions contributing to cyclone formation (Anandh *et al*., 2018; 2020) and the ability to model and predict how these conditions may evolve progressively. Seasonal dynamics in ocean communities can affect various surface features, such as temperature, salinity, nutrient concentrations, and oxygen levels, which may affect populations of phytoplankton and marine organisms. These variations in ocean surface features, including temperature, nutrient availability, and currents, can significantly impact marine ecosystems and their productivity. Such changes can inadvertently disturb the growth and distribution of phytoplankton, the base of the marine food web, and in turn, upset the entire ecosystem. The ocean community models' influence on these surface features was investigated by reviewing the literature and analyzing models. Key environmental factors driving the changes in ocean communities and surface features, such as temperature, nutrient availability, and ocean currents, were also identified. Seasonal surface features in coastal and regional ocean environments, such as sea surface temperature, currents, and wind patterns, can significantly impact ocean-atmosphere interactions and climate patterns. Also known as air-sea interactions, these involve the exchange of energy, heat, and moisture between the ocean and the atmosphere. The study aims to understand the sensitivity of the upper BoB by analyzing surface variables, temperature, salinity, and other parameters using model simulations to explore seasonal variability. This study was carried out in India's BoB region using the numerical model simulation in 2022.

MATERIALS AND METHODS

Numerical model, data, and methodology

The Coastal and Regional Ocean COmmunity (CROCO) is a state-of-the-art numerical ocean model that simulates the dynamics of coastal and regional ocean systems. The CROCO model is based on the Regional Ocean Modeling System (ROMS), a free-surface, terrain-following, hydrostatic, primitive equation ocean model. It was developed as an extension of the ROMS model to include a range of physical and biogeochemical processes important for simulating coastal and regional ocean systems. The model has been applied to various research problems, including coastal erosion, oil spill modeling, and marine ecology. The CROCO is a hybrid model that combines the primitive equations of ocean dynamics with a free surface and a hydrostatic assumption and includes various parameters of physical processes such as turbulence, mixing, and surface fluxes. These parameterizations are based on empirical relationships and theoretical model approaches. The CROCO modeling system estimates the ocean and atmospheric state of the BoB. The model is based on a stretched terrain-following hydrostatic approach designed to solve the momentum and primitive equations at high resolution. The Arakawa C-grid, staggered horizontally, is employed to solve primitive equations. It also includes finite-discretized coastal boundaries acquired through a sea/land mask. An accurate representation of coastal dynamics, such as coastal upwelling and downwelling, and mixing processes, requires the inclusion of coastal boundaries. The CROCO model is a powerful tool for simulating ocean dynamics in coastal and regional areas. Also, the model's high resolution and accurate representation of coastal boundaries make it particularly useful for studying the BoB. A regional model of the BoB region was established, covering a range of latitudes 4˚N to 24˚N and longitudes 72˚E to 100˚E. The model comprised a grid of 256 x 249 horizontal surface points, providing an estimated resolution of 10 kilometers (km). While the northern, eastern, and a significant portion of the western boundaries were closed, the southern boundary was left open. The Levitus monthly climatology was employed to facilitate the temperature and salinity values on the open boundary. In contrast, the model utilized 32 S-coordinate layers in the vertical and incorporated Earth Topography 2–minutes (ETOPO2) data to establish the bottom topography. The study area is illustrated in Fig. 1. his study entailed an 8-year climatological simulation using the CROCO model. A 3-year spin-up period was also performed to examine the monthly variability of the ocean's upper surface in the bay. Additionally, simulations were conducted for monthly analyses of the salinity, temperature, depth of the 20˚C and 26˚C Isothermal Layer (D20 and D26), and net heat flux. This study's methodology ensured that the model produced reliable results, which were used to gain insights into the dynamics of the ocean-atmosphere system in the BoB. Figs. 2 and 3 show the volume-averaged salt content and temperature outputs from the CROCO model. Both results demonstrate that the model stabilized from the second year onward.

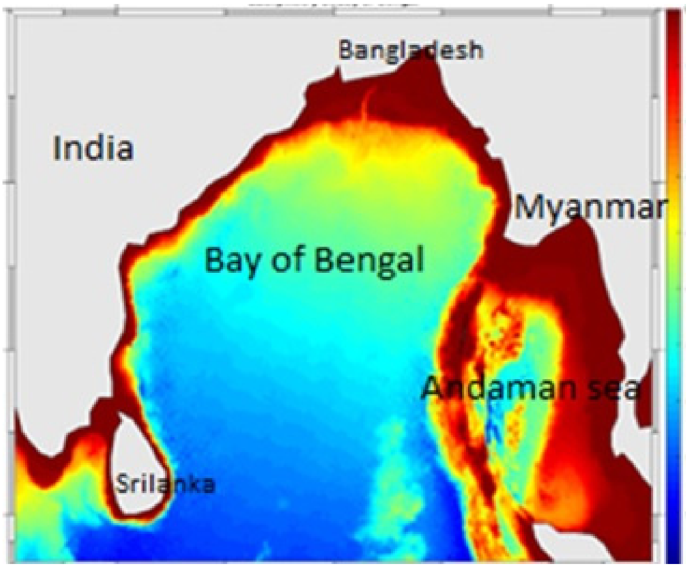

Fig. 1: Geographical location of the study area in the Bay of Bengal in India

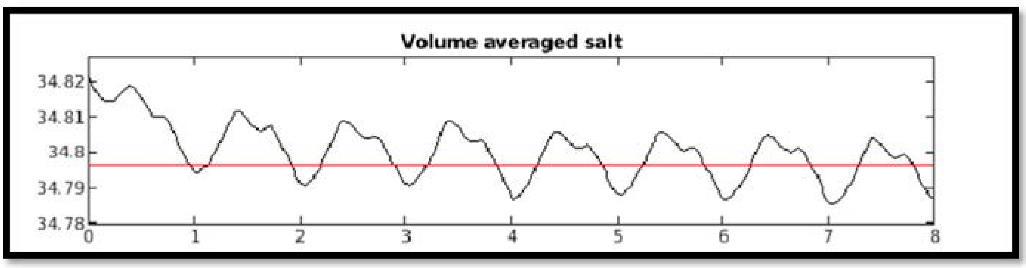

Fig. 2: Volume averaged salt for 8 years

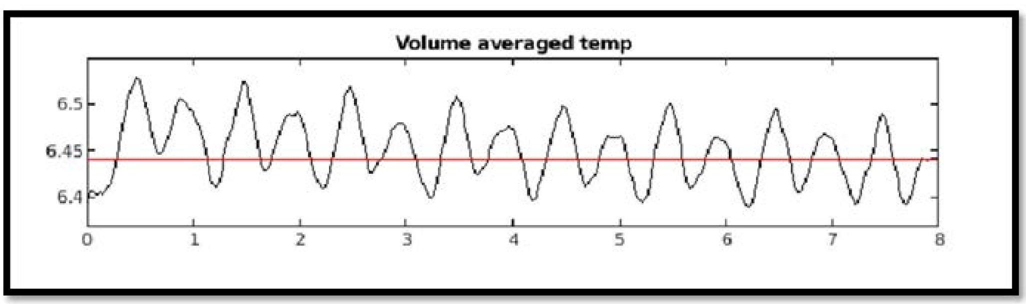

Fig. 3: Volume averaged temperature for 8 years

RESULTS AND DISCUSSION

Sea surface temperature (SST)

The surface temperature of the BoB varies significantly throughout the year, with the western region experiencing high temperatures during certain months. Fig.4 demonstrates the monthly climatological variations of SST. During the winter, the SST ranges from 26 °C to 29 °C throughout the bay, with the south and east experiencing higher temperatures. During the pre-monsoon months of March to May, the temperature in all three bay regions is the highest, ranging from 29 °C to 32 °C.

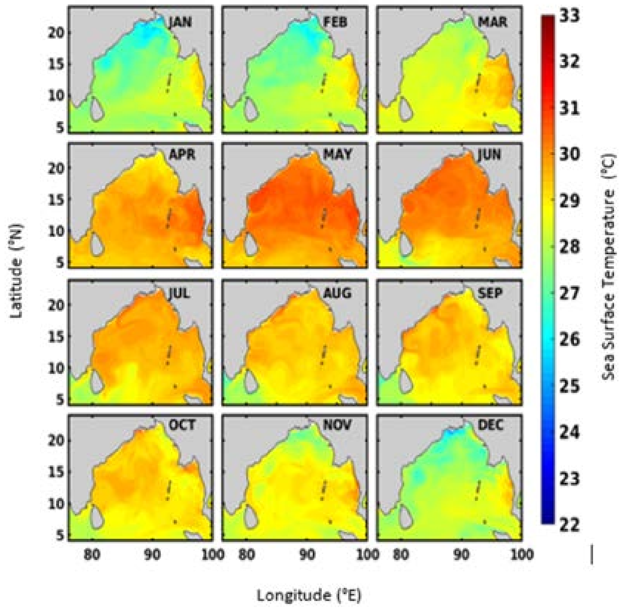

Fig. 4: Monthly climatological variations of sea surface temperature (°C)

In March, the temperature ranges from 27 °C to 31°C, with the central bay presenting a 1°C bias. In April, the temperature ranges from 29 °C to 30 °C, and this increase in temperature causes cyclones to intensify when they cross near the western coast. In May, the western coast experiences the highest temperatures of 30 °C to 32 °C, while the northern, eastern, and southern coastal areas range from 29 °C to 30 °C. In the central bay region, the temperature ranges from 30 °C to 31 °C. During the monsoon season (June to September), the temperature in the western, northern, and eastern bays ranges from 30 °C to 32 °C in June, influenced by the summer season. Due to rainfall from July to September, the surface and subsurface temperatures become cooler, ranging from 29°C to 30°C in the northern, eastern, and western bay regions. In contrast, the south bay region experiences temperatures ranging from 29 °C to 27 °C at the bottom tip. According to Girishkumar and Ravichandran (2012), the pre-and post-monsoon seasons over the bay are characterized by high sea surface temperatures and winds, resulting in frequent air-sea interactions that facilitate the formation and development of cyclones during these periods.

Sea surface salinity (SSS)

The monthly climatological variations in salinity are represented in Fig. 5. During the winter season (December to February), the salinity in the northern and eastern regions of the BoB has a low range of 30-31 Practical Salinity Unit (psu), while in the western bay, it ranges from 33 to 34 psu, and in the southern bay, it reaches its highest values of 34-35 psu. These values represent the post-monsoon conditions; there is no rainfall contribution, but the after-effects of the monsoon rains can still be perceived in the northern bay's low salinities. In the pre-monsoon season (March to May), the northern and eastern bay regions' salinity ranges around 31–32 psu. The salinity distribution ranges from 33 to 34 psu in the southern and central regions, with a bias of 1 psu in the central bay and the western region. During the pre-monsoon season, the sea surface salinity increases due to the relative minimum freshwater flow. The influx of freshwater still affects salinity, but cool and dry air over the bay reduces evaporation (Dandapat *et al*., 2021) and mixes fresh water with salt water. Even though freshwater from rivers is not included, the models show a reduction in surface salinity during monsoon months owing to rainfall and moisture flux. In June, the salinity in the northern and eastern bay regions ranges from 30 to 32 psu, from 33 to 34 psu in the central bay, from 33 to 35 psu in the southern bay, and from 33 to 35 psu in the western

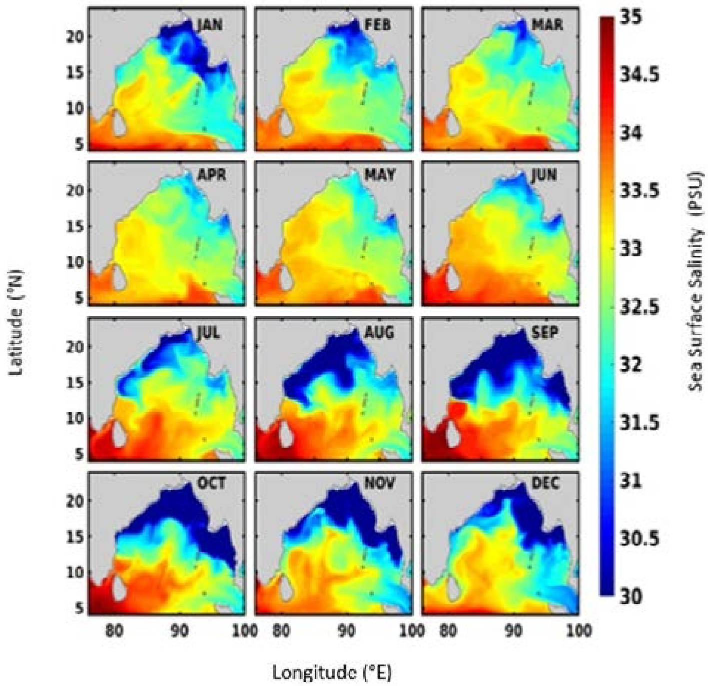

Fig. 5: Monthly Climatological Variations of Sea Surface Salinity (PSU)

bay. In July, the salinity in the northern, eastern, and western bay regions ranges from 30 to 32 psu, while in the southern bay, it ranges from 33 to 35 psu. The central bay's salinity ranges at 33 psu. During the monsoon season, freshwater starts impacting the western bay. In August, the salinity in the northern and western boundaries ranges from 30 to 32 psu, while the southern bay exhibits the highest salinities at 33–34 psu. In September, the northern, eastern, and southern bays range from 30 to 32 psu due to river water mixing in the ocean from rainfall and moisture flux. In the central bay, there is a mixing of 31 to 33 psu. Similar to September, the monsoon's influence in October causes slight changes in the central bay, ranging from 32 to 33 psu with a bias of 1 psu. In November (winter season), the lowest salinity of 30-31 psu is observed in the northern and eastern bay, while in the central bay, it ranges at 32 psu due to eddies. The surface salinity during monsoons these low in the north and the western and eastern boundaries, about 15°N. This information has been obtained from a previous study (Chakraborty and Gangopadhyay, 2016).

Isothermal layer depth (D20)

The isothermal layer depth is a substitute for the thermocline. The isothermal layer depths D20 and D26 are critical indicators of the extensions of surface eddies in the deep waters of the BoB. These eddies can store significant amounts of heat energy that can affect the oceanic environment and potentially influence cyclones passing over them. Deep warm eddies in the west side of the BoB can persist for up to 9 months, impacting the overall oceanic conditions. The monthly climatological variations in the isothermal layer at D20 are shown in Fig. 6. During the winter months (December, January, and February), D20 depths range from 60 m to 180 m across the BoB region. There is also a sudden temperature reversal along India's east coast from December to January. In the central bay, D20 depths can reach up to 180 m, with surface eddies extending to the deep waters. As winter progresses into spring, surface eddies are observed to extend deeper into the western bay areas, reaching depths of 180 m to 200 m. In the northern and southern bay regions, eddies are observed at depths of 100 m to 140 m,

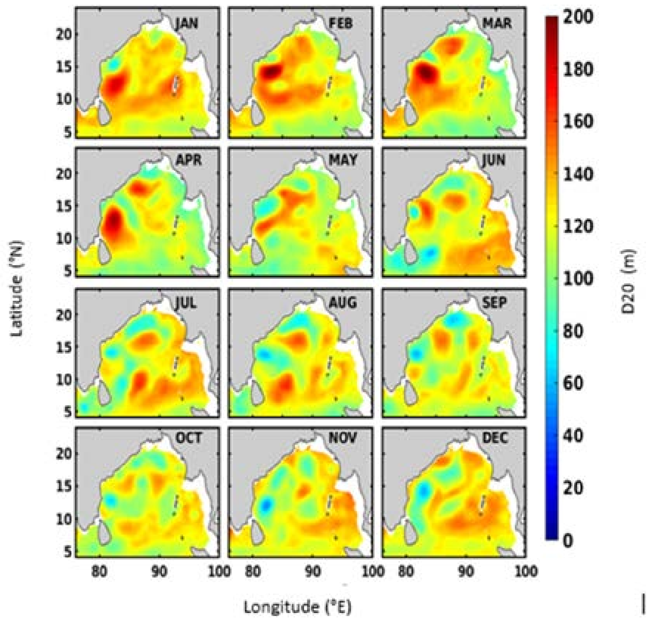

Fig. 6: Monthly Climatological Variations of the Isothermal Layer Depth D20 (m)

while in the central bay, they can reach up to 200 m. D20 depths remain relatively stable in March and April, ranging from 80 m to 120 m in the northern, eastern, and southern bay regions and from 140 m to 200 m in the western bay region. Surface eddies along the western bay extend to even deeper waters until April, storing significant amounts of heat energy. The D20 layer starts shifting to shallower depths with the onset of monsoon except near the deepest regions of the bay. A report has presented a distinctive feature of the BoB: forming a basinwide subsurface cyclonic gyre from June to November and an anticyclonic gyre from December to May (Sil and Chakraborty, 2012).

Isothermal layer depth (D26)

In the winter (December to February), the D26 depth of the isothermal layer ranges from 40 m to 80 m below the surface, with the western bay at 40 m to 80 m and the central bay at 80 m to 100 m deep. The surface eddies extend into deeper waters near the bay's western boundary, storing more heat energy. November–December marks the region's cyclone season. Fig. 7 shows the monthly climatological variations of D26. In February, the D26 depth ranges from 100 m to 120 m in the central region, while the western bay experiences warm eddies up to April, even at 120 m depth or more. In March, the D26 depth ranges from 40 m to 80 m in the northern, eastern, and southern bay regions and from 80 m to 120 m in the western bay region. With the surface temperatures increasing in April, the D26 gets shallower except in the western boundary, where it stays at more than 100 m depth. It may be noted that April is also the beginning of cyclone season in this region. In May, the depth ranges from 60 m to 40 m throughout, except in the west-central region where the D26 is slightly deeper, at 80 m to 100 m depth. From June to September, the D26 of the BoB almost divides into two distinct regions, the western boundary (D26 < 60 m) and the central and eastern regions (D26 > 80 m or more). The D26 continues to get shallower through October and November except in the south and east. It has been reported that (Swain and Navaneeth Krishnan, 2013) during the inter-monsoon period spanning October and November, a significant portion of the North Indian Ocean experiences low wind speeds and relatively low net heat loss, and moderate peak radiation during the day. These combined factors contribute to the shallow depth of the D26 thermocline, typically less than 60 m in most parts of the North Indian Ocean during this period.

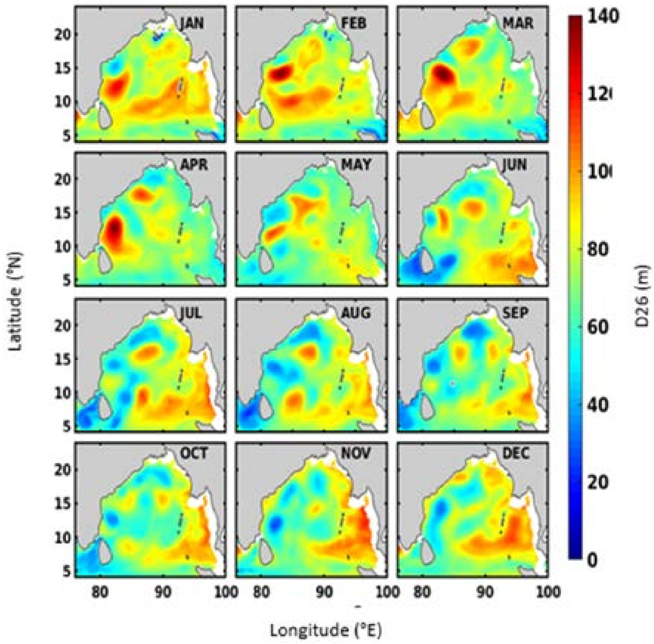

Fig. 7: Monthly climatological variations depth of the isothermal layer D26 (m).

Net heat flux

The net heat flux refers to the exchange of heat between the atmosphere and the ocean, affecting the atmospheric and oceanic processes and their interaction within the ocean-atmosphere system. Previous studies have indicated that theworld's oceans' mixed layer depth (MLD) is affected by external local forces, such as net heat flux (Evaporation minus precipitation plus wind stress). Heat transferred into the ocean is considered positive for downward flux, while heat released from the ocean is considered negative for upward flux. Fig. 8 displays the monthly climatological variations of net heat flux. Throughout the pre-monsoon season (March-May), the net heat flux is positive and ranges from 50 to 100 W/m^2 in all four bay regions (North, East, South, and West), with the maximum exchange occurring due to shortwave radiation. In May, slight changes are observed in the heat flux of the western and northern bay regions, where the range remains 50 to 100 W/m^2, whereas the heat flux from the eastern bay ranges from 0 to 50 W/m^2. The southern bay experiences a heat flux of approximately 50 W/m^2, attributable to the negative latent heat flux occurring at the interface of the atmosphere and ocean. This phenomenon also contributes to the negative Qnet. In the monsoon season (June to September), the net heat flux ranges from 0 to 100 W/m^2 in the western boundary, with negative values noted in June and July due to upward longwave radiation flux. Only the south bay region ranges negatively in August and September, with upward flux contributing more to the net heat flux. In the post-monsoon season (October and November), the heat transmitted into the ocean results in a positive net heat flux due to downward flux in the western, northern, and eastern bays. A mix of negative and positive values is observed in the central and southern bays due to latent heat flux. In the winter, the net heat flux ranges from 0 to -100 W/m^2 in December and January, with heat stored in the subsurface due to upward flux. Heat is diffused from the ocean and liberated in February as a positive heat range in all four bay areas. The North BoB experiences a maximum deepening of minus 50 m during winter, notably characterized by the negative net heat flux, with negative latent heat flux at the atmosphere-ocean interface contributing significantly to the negative Qnet. The North BoB experiences a maximum deepening of ~ 50 meters in the winter monsoon season. This deepening can be primarily attributed to the dominance of negative Qnet in the North BoB (Sadhukhan *et al*., 2021).

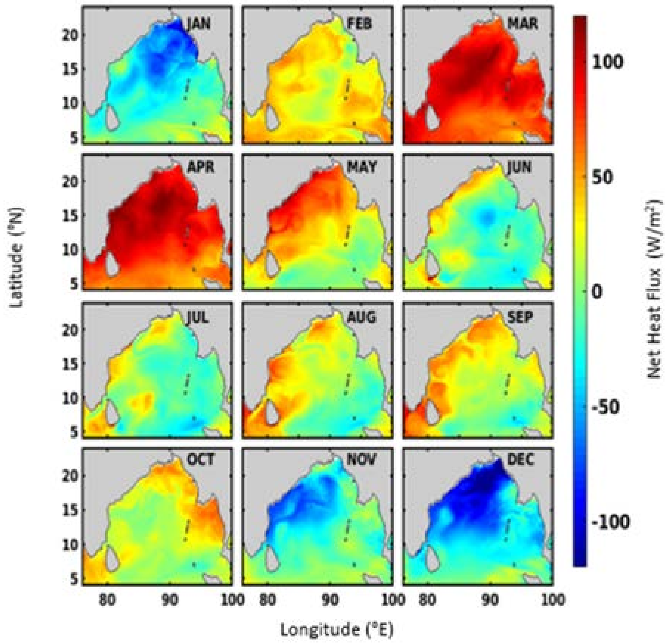

Fig. 8: Monthly climatological variations net heat flux (W/m^2)

CONCLUSION

The numerical model CROCO was utilized to establish a regional model for the BoB covering an area ranging from 4˚N to 24˚N in latitude and 72˚E to 100˚E in longitude. The model comprised a grid of 256 x 249 horizontal surface points, providing an estimated resolution of 10 km. ETOPO2 was used for the model bathymetry and Levitus climatology to assess the temperature and salinity of the open boundaries. The simulation demonstrated higher sea surface temperatures in the BoB, with a value of 28 °C or higher for most of the year, except during winter. The onset of the monsoon season was observed to cause a reduction in the surface salinity in the north, west, and eastern boundaries. Apart from the bay's deepest regions, the D20 layer shifted towards shallower depths with the onset of monsoon. This shift can be attributed to the significant amount of freshwater input during the monsoon season, which reduces the density of the surface waters, causing them to rise and mix with the underlying waters. Additionally, the D26 layer became shallower from October through November, except in the south and east, which may be caused by the cooling of the surface waters during this period, increasing their density and causing them to sink, leading to the shoaling of the D26 layer. During winter, the northern BoB experienced negative net heat flux, which was reversed before the onset of the monsoon. This reversal is due to the atmospheric circulation changes associated with the monsoon season, which leads to heat transfer from the atmosphere to the ocean, resulting in a positive net heat flux. The findings of this study provide important insights into the physical processes governing the surface characteristics of the BoB. Using the CROCO model, accurately simulating the BoB's surface features, including salinity, temperature, D20, D26, and net heat flux, contributed to a better understanding of the region's dynamics. These conclusions contribute to a good understanding of the surface characteristics in the BoB and can aid in predicting its future behavior, particularly regarding climate change and sea level rise, and can inform the development of effective adaptation and mitigation strategies. Global warming causes increased global temperatures and heat, 90 % of which is transferred to the ocean, and the rest of the 10 % is transferred to air and land. Given the earlier study demonstrating a global increase in heat in the air, land, and sea, a climatological study is vital to raise societal awareness.

AUTHOR CONTRIBUTIONS

D. Jaishree performed the literature review, preprocessing for simulations, processing model output, and data analysis, prepared the manuscript text and edition. P.T. Ravichandran contributed to the supervision of the work and preparation of the manuscript. V. Deeptha Thattai contributed to the conceptualization, pre-processing, data analysis, and manuscript review for publication.

ACKNOWLEDGEMENT

The first author expresses gratitude to the Indian Institute of Technology Kharagpur for facilitating and providing the CORAL laboratory for simulation. Sincere thanks are extended to Arun Chakraborty and Anandh TS for their valuable suggestions and discussions.

CONFLICT OF INTEREST

The author declares that there is no conflict of interest regarding the publication of this manuscript. In addition, the ethical issues, including plagiarism, informed consent, misconduct, data fabrication and falsification, double publication and submission, and redundancy, have been completely observed by the authors.

OPEN ACCESS

PUBLISHER'S NOTE

GJESM Publisher remains neutral with regard to jurisdictional claims in published maps and institutional affiliations.

ABBREVIATIONS

%	Percent
°C	Degree Celsius
BoB	Bay of Bengal
CROCO	Coastal and Regional Ocean COmmunity model
D20	Depth of the Isothermal Layer-D20
D26	Depth of the Isothermal Layer-D26
ETOPO2	Earth TOPOgraphy 2–minutes
km	Kilometer
Km^2	Square Kilometer
m	Meter
psu	Practical Salinity Unit
SSS	*Sea surface salinity*
SST	Sea Surface Temperature
W/m^2	Watt per square meter

REFERENCES

Akhter, S.; Qiao, F.; Wu, K.; Yin, X.; Chowdhury, K.M.A.; Chowdhury, N.U.M.K., (2021). Seasonal and long-term sea-level variations and their forcing factors in the northern Bay of Bengal: A statistical analysis of temperature, salinity, wind stress curl, and regional climate index data. Dyn. Atmos. Oceans. 95: 1-23 **(23 Pages)**.

Ali, M.M.; Jagadeesh, P.S.V.; Jain, S., (2007). Effects of eddies on Bay of Bengal cyclone intensity. Eos. 88(8): 93-104 (**12 Pages).**

Amsalia, N.; Haditiar, Y.; Wafdan, R.; Ikhwan, M.; Chaliluddin, M.A.; Sugianto, S.; Rizal, S., (2022). The currents, sea surface temperature, and salinity patterns in the Bay of Bengal. E3S Web of Conferences. 339 02001: 1–7 **(7 Pages).**

Anandh, T.S.; Das, B.K.; Kumar, B.; Kuttippurath, J.; Chakraborty, A., (2018). Analyses of the oceanic heat content during 1980–2014 and satellite-era cyclones over Bay of Bengal. Int. J. Climatol., 38(15): 5619 –5632 **(14 Pages).**

Anandh, T.S.; Das, B.K.; Kuttippurath, J.; Chakraborty, A., (2020). A coupled model analyses on the interaction between oceanic eddies and tropical cyclones over the Bay of Bengal. Ocean Dyn., 70: 327-337 **(11 Pages).**

Bartzokas, A.; Metaxas, D.A.; Giles, B.D., (2018). On the relation between sea surface and lower temperature over the northern hemisphere. Global NEST J., 4(2): 127–137 **(11 Pages).**

Chakraborty, A.; Gangopadhyay, A., (2016). Development of a high-resolution multiscale modeling and prediction system for Bay of Bengal, Part I: climatology-based simulations. Open J. Mar. Sci., 6: 145–176 **(32 Pages).**

Cherian, D.A.; Shroyer, E.L.; Wijesekera, H.W.; Moum, J.N., (2020). The seasonal cycle of upper-ocean mixing at 8°N in the Bay of Bengal. J. Phys. Oceanogr., 50(2): 323–342 **(20 Pages)**.

Dandapat, S.; Chakraborty, A.; Kuttippurath, J.; Bhagawati, C.; Sen, R., (2021). A numerical study on the role of atmospheric forcing on mixed layer depth variability in the Bay of Bengal using a regional ocean model. Ocean Dyn., 71: 963–979 **(17 Pages).**

Dyn, C., (2010). The Indian summer monsoon Pre-onset land surface processes and 'internal' interannual variabilities of the Indian summer monsoon. Clim. Dyn., 36: 2077–2089 **(13 Pages).**

Echols, R.; Stephen C. Riser., (2020). The impact of barrier layers on arabian sea surface temperature variability. Geophys. Res. Lett., 47(3): 1–9 **(9 Pages).**

Fan, K.; Wang, X.; He, Z., (2020). Control of salinity estratification on recent increase in tropical cyclone intensification rates over the post-monsoon Bay of Bengal. Environ. Res. Lett., 15(9): 1-10 **(10 Pages).**

Girishkumar, M.S.; Ravichandran, M., (2012). The influences of ENSO on tropical cyclone activity in the Bay of Bengal during October-December. J. Geophys. Res. C: Oceans. 117(C2): 1–13 **(13 Pages).**

Gordon, A.L.; Mahadevan, A.; Hole, W.; Sengupta, D., (2016). Bay of Bengal: 2013 Northeast monsoon upper-ocean circulation. Oceanography. 29(2): 82-91 **(10 Pages).**

Horii, T.; Ueki, I.; Ando, K.; Hasegawa, T.; Mizuno, K.; Seiki, A., (2016). Impact of intraseasonal salinity variations on sea surface temperature in the eastern equatorial indian ocean. J. Oceanogr., 72: 313–326 **(14 Pages).**

Jongaramrungruang, S.; Seo, H.; Ummenhofer, C.C., (2017). Intraseasonal rainfall variability in the Bay of Bengal during the Summer Monsoon: coupling with the ocean and modulation by the Indian Ocean Dipole. Atmos. Res. Lett., 18(2): 88–95 **(8 Pages).**

Jourdain, N.C.; Lengaigne, M.; Vialard, J.R.; Madec, G.; Menkes, C.E.; Vincent, E.M.; Jullien, S.; Barnier, B., (2013). Observation-based estimates of surface cooling inhibition by heavy rainfall under tropical cyclones. J. Phys. Oceanogr., 3(1): 1-17 **(17 Pages).**

Jyothi, L.; Joseph, S.; Suneetha, P., (2019). Surface and Sub-surface Ocean Response to Tropical Cyclone Phailin: Role of Pre-existing Oceanic Features. J. Geophys. Res. C: Oceans. 124(9): 6515-6530 **(16 Pages).**

Kawai, Y.; Wada, A., (2007). Diurnal sea surface temperature variation and its impact on the atmosphere and ocean: A review. J. Oceanogr., 63: 721–744 **(24 Pages).**

Kikuchi, K.; Wang, B.; Fudeyasu, H., (2009). Genesis of tropical cyclone nargis revealed by multiple satellite observations. Geophys. Res. Lett., 36(6): 1–5 **(5 Pages).**

Kodunthirapully Narayanaswami, N.; Ramasamy, V., (2022). Tropical cyclone intensity modulated by the oceanic eddies in the Bay of Bengal. Oceanologi., 4(3): 445-456 **(12 Pages).**

Krishnamurti, T.N.; Jana, S.; Krishnamurti, R.; Kumar, V.; Deepa, R.; Papa, F.; Bourassa, M. A.; Ali, M.M., (2017). Monsoonal intraseasonal oscillations in the ocean heat content over the surface layers of the Bay of Bengal. J. Mar. Syst., 167: 19–32 **(14 Pages).**

Lee, C.M.; Jones, B.H.; Brink, K.H.; Fischer, A.S., (2000). The upper-ocean response to monsoonal forcing in the Arabian Sea: seasonal and spatial variability. Deep Sea Res. Part II. 47(7-8): 1177–1226 **(50 Pages).**

Li, Y.; Han, W.; Hu, A.; Meehl, G.A.; Wang, F., (2018). Multidecadal changes of the upper Indian ocean heat content during 1965-2016. J. Clim., 31(19): 7863–7884 **(22 Pages).**

Lin, I.I.; Chen, C.H.; Pun, I.F.; Liu, W.T.; Wu, C.C., (2009). Warm ocean anomaly, air sea fluxes, and the rapid intensification of tropical cyclone Nargis (2008). Geophys. Res. Lett., 36(3): 2–6 **(5 Pages).**

Maneesha, K.; Ravichandran, M.; Yu, W., (2012). Upper ocean variability in the Bay of Bengal during the tropical cyclones Nargis and Laila. Prog. Oceanogr., 106: 49-61 **(13 Pages).**

Oldemar de Oliveira Carvalho-Junior, (2022). Salinity in the surface of the indian ocean. Mar. Sci., 2022. 10(1): 1–8 **(8 Pages).**

Potemra, J.T.; Luther, M.E.; O'Brien, J.J., (1991). The seasonal circulation of the upper ocean in the Bay of Bengal. J. Geophys. Res. C: Oceans. 96(C7): 12667-12683 **(17 Pages).**

Roy Chowdhury, R.; Prasanna Kumar, S.; Chakraborty, A., (2021). Simultaneous occurrence of tropical cyclones in the northern indian ocean: Differential response and triggering Mechanisms. Front. Mar. Sci., 8: 1-25 **(25 Pages).**

Sadhukhan, B.; Chakraborty, A.; Kumar, A., (2021). Role of external forcing on the seasonal and interannual variability of mixed layer depth over the Bay of Bengal using reanalysis datasets during 1980–2015. Dyn. Atmos. Oceans., 93: 1-13 **(13 Pages).**

Salathe Jr, E.P.; Steed, R.; Mass, C.F.; Zahn, P.H., (2008). A high-resolution climate model for the US Pacific Northwest: Mesoscale feedbacks and local responses to climate change. J. Clim., 21: 1–24 **(24 Pages).**

Sardessai, S.; Ramaiah, N.; Prasanna Kumar, S.; De Sousa, S.N., (2007). Influence of environmental forcings on the seasonality of dissolved oxygen and nutrients in the Bay of Bengal. J. Mar. Res., 65: 1-25 **(25 Pages).**

Schott, F.A.; McCreary, J.P., (2001). The monsoon circulation of the indian ocean. Prog. Oceanogr., 51(1): 1-123 **(123 Pages).**

Sen, R.; Francis, P.A.; Chakraborty, A.; Effy, J.B., (2021). A numerical study on the mixed layer depth variability and its influence on the sea surface temperature during 2013 – 2014 in the Bay of Bengal and equatorial indian ocean. Ocean Dyn., 71: 527-543 **(17 Pages).**

Segele, Z.T.; Lamb, P.J.; Leslie, L.M., (2009). Large-scale atmospheric circulation and global sea surface temperature associations with horn of Africa June-September rainfallInt. J. Climatol., 29(8): 1075–1100 **(26 Pages).**

Setiawan, R.Y.; Iskandar, I.; Wirasatriya, A.; Dwi Susanto, R.; Siswanto, E.; Pranowo, W.S.; Setiawati, M.D.; Mardiansyah, W., (2022). Seasonal and interannual coastal wind variability off the central Maluku Islands revealed by satellite oceanography. Global Nest J., 24(1): 37–43 **(7 Pages).**

Sharada, M.K.; Devasena, C.K.; Swathi, P.S.; SundaraDeepthi, M.V.; ShelvaSrinivasan, M.K.; Yajnik, K.S., (2015). Seasonal and interannual variability of marine ecosystem in the north indian Ocean: A model evaluation study. The Int. J. Ocean Clim. Syst., 6: 19–34 **(16 Pages).**

S. Sil, S.; Chakraborty, A., (2012). The Mechanism of the 20°C Isotherm depth oscillations for the Bay of Bengal, Mar. Geod., 35(3): 233–245 **(13 Pages).**

Suprit, K.; Neelakandan, S.K., (2016). What controls seasonal evolution of sea surface temperature in the bay of bengal? mixed layer heat budget analysis using moored buoy observations along 90°E. oceanography. 29(2): 202-213 **(12 Pages).**

Swain, D.; V. C. Navaneeth Krishnan, V.C., (2013). (2013). Prediction of depth of 26 °C isotherm and tropical cyclone heat potential using a one-dimensional ocean model. (1): 1-28 **(28 Pages).**

Thadathil, P.; Gopalakrishna, V.V.; Muraleedharan, P.M.; Reddy, G.V.; Araligidad, N.; Shenoy, S., (2002). Surface layer temperature inversion in the Bay of Bengal. Deep Sea Res. Part I. 49(10): 1801–1818 **(18 Pages).**

Ts, A.; Das, B.K.; Kuttippurath, J.; Chakraborty, A., (2020). A coupled model analyses on the interaction between oceanic eddies and tropical cyclones over the Bay of Bengal. Ocean Dyn., 70: 327-337 **(11 Pages).**

Vecchi, G.A.; Harrison, D.E., (2002). Monsoon breaks and subseasonal sea surface temperature variability in the Bay of Bengal. J. Clim., 15(12): 1485–1493 **(9 Pages).**

Vinayachandran, P.N.; Jr, J.P.M.; Hood, R.R.; Kohler, K.E., (2014). Numerical investigation of the phytoplankton bloom in the Bay of Bengal during northeast monsoon. J. Geophys. Res., 110(C12): 1-14 **(14 Pages).**

Wainer, I.; Webster, P.J., (1996). Monsoon/El Nino-southern oscillation relationships in a simple coupled ocean-atmosphere model. J. Geophys. Res. C: Oceans. 101(C11): 25599-25614 **(16 Pages).**

Webster, P.J.; Magaña, V.O.; Palmer, T.N.; Shukla, J.; Tomas, R.A.; Yanai, M.; Yasunari, T., (1998). Monsoons: processes, predictability, and the prospects for prediction. J. Geophys. Res. C: Oceans. 103(C7): 14451–14510 **(60 Pages).**

Yadav, M., (2022). South Asian monsoon extremes and climate change, in: Saxena, P., Shukla, A., Gupta, A.K. (Eds.), Extremes in Atmospheric Processes and Phenomenon: Assessment, Impacts and Mitigation. Springer Nature Singapore, Singapore. 59–86 **(28 Pages).**

Yoo, S.H., Fasullo, J., Yang, S., Ho, C.H., (2010). On the relationship between Indian Ocean Sea surface temperature and the transition from El Nio to la Niña. J. Geophys. Res. D: Atmos., 115(D15): 1–20 **(20 Pages).**

Yu, L., Hole, W., (2015). Ocean preconditioning of cyclone nargis in the Bay of Bengal: Interaction between rossby waves, surface fresh waters and sea surface temperatures. J. Phys. Oceanogr., 41(9): 1741-1755 **(15 Pages).**

AUTHOR (S) BIOSKETCHES

Jaishree, D., Ph.D. Candidate, Assistant Professor, Department of Civil Engineering, Faculty of Engineering and Technology, SRM Institute of Science and Technology, Kattankulathur - 603203, Chengalpattu District, Tamil Nadu, India.

- Email: *jaishred@srmist.edu.in*
- ORCID: 0000-0003-0401-068X
- Web of Science ResearcherID: NA
- Scopus Author ID: 57193997236
- Homepage: https://www.srmist.edu.in/faculty/jaishree-d-2/

Ravichandran, P.T., Ph.D., Professor, Head of the Department of Civil Engineering, Faculty of Engineering and Technology, SRM Institute of Science and Technology, Kattankulathur - 603203, Chengalpattu District, Tamil Nadu, India.

- Email: *ravichap@srmist.edu.in*
- ORCID: 0000-0002-9555-2005
- Web of Science ResearcherID: NA
- Scopus Author ID: 23493524100
- Homepage: https://www.srmist.edu.in/faculty/dr-p-t-ravichandran/

Thattai, D.V., Ph.D., Independent Researcher. Adyar, Chennai, Tamil Nadu, India.

- Email: *vtdeeptha@gmail.com*
- ORCID: 0000-0001-9121-7106
- Web of Science ResearcherID: NA
- Scopus Author ID: 6506859341
- Homepage: https://scholar.google.com.tw/citations?user=1UTy2sIAAAAJ&hl=en

HOW TO CITE THIS ARTICLE

Jaishree, D.; Ravichandran, P.T.; Deeptha Thattai, D.V., (2023). Exploring the dynamics of seasonal surface features using coastal and regional ocean community model. Global J. Environ. Sci. Manage., 9(4): 741-752.

DOI: 10.22035/gjesm.2023.04.06

URL: https://www.gjesm.net/article_704449.html